Available online at www.sciencedirect.com
ScienceDirect
Scripta Materialia 60 (2009) 281–284
Scripta MATERIALIA
www.elsevier.com/locate/scriptamat

Investigation of the dwell period's influence on the fatigue crack growth of a titanium alloy

P. Lefranc,[a,b,c] C. Sarrazin-Baudoux,[a,*] V. Doquet[b] and J. Petit[a]

[a] *LMPM, UMR CNRS 6617, ENSMA, 86961 Futuroscope Chasseneuil Cedex, France*
[b] *LMS, UMR CNRS 7649, Ecole Polytechnique, 91128 Palaiseau Cedex, France*
[c] *SNECMA Groupe SAFRAN, 77550 Moissy Cramayel, France*

Received 15 February 2008; revised 13 September 2008; accepted 19 September 2008
Available online 26 October 2008

The dwell effect, which is known to induce a reduction in the fatigue life of titanium alloys at room temperature, is related to early crack initiation. The present results support faster crack growth rates. The governing mechanisms are identified by mean of scanning electron microfractographic observations. The potential role of the atmosphere is examined through comparative testing performed in air and in high vacuum in order to distinguish the specific contributions of cold creep and environment assistance.

Keywords: Titanium alloy; Dwell fatigue; Fatigue; Crack growth

Due to their attractive mechanical properties even at temperatures ranging up to 600 °C, titanium alloys are used by the aeroengine industry to manufacture gas turbine and compressor discs. However, since 1972, engineers have come up against the so-called dwell effect, a phenomenon consisting of a reduction in fatigue life at room temperature due to the introduction of hold periods at the peak stress of the cyclic loading waveform. To date, the problem has remained an open one from both the scientific and engineering points of view.

Several authors have studied the dwell effect on the crack growth rate of titanium alloys, with contrasting results. On the one hand, some of them [1–4] did not observe any deleterious effect on crack propagation kinetics due to the introduction of dwell periods. Because of this, Eylon and Hall [1] attributed the dwell life debit only to an earlier crack initiation. According to Bania and Eylon [2], dwell periods might reduce the crack growth rate as a result of the high crack path tortuosity induced by the dwell-fatigue loading. On the other hand, other authors [5–6] noticed an increase in the crack growth rate under dwell loading. According to Stubbington and Pearson [5], dwell periods enhanced the crack growth rate when the crack propagated in or near the basal plane. Evans and Gostelow [6] attributed a similar deleterious effect to a time-dependent accumulation of strain, which is enhanced by internal hydrogen due to an ageing effect. Finally, another study [7] showed an earlier crack initiation under dwell loading but did not answer the question of the dwell effect on crack propagation. To gain a deeper understanding of the mechanisms governing the reduction in fatigue life associated with the dwell effect, this paper studies the influence of dwell periods on crack growth in a Ti-6242 alloy as compared to fatigue crack propagation under cyclic fatigue.

The material used in this study was a Ti–6Al–2Sn–4Zr–2Mo (Ti-6242) alloy. The heat treatment consisted of a forging above the beta transus, inducing a purely lamellar microstructure. To analyse the microstructure, small specimens were extracted from the blank, then mechanically polished with emery paper and finally polished with diamond paste. After polishing, Kroll's reagent (1–3 ml of HF, 2–6 ml HNO_3 in 100 ml of H_2O) was used to reveal the microstructure.

Scanning electron microscopy (SEM) observations showed a high level of microstructural heterogeneity, resulting from the thermomechanical treatments performed after the forging. The microstructure was characterized by a mixture of either Basketweave (Fig. 1a) or Windmanstätten areas (Fig. 1b) in prior β grains (Fig. 1c). In all cases the average width of the lamellas was around 2.5 mm and the size of the β grains was about 200 μm.

The crack growth rate tests were performed on a servo-hydraulic testing machine of 20 kN capacity. All tests

* Corresponding author. E-mail: baudoux@lmpm.ensma.fr

1359-6462/$ - see front matter © 2008 Acta Materialia Inc. Published by Elsevier Ltd. All rights reserved.
doi:10.1016/j.scriptamat.2008.09.033

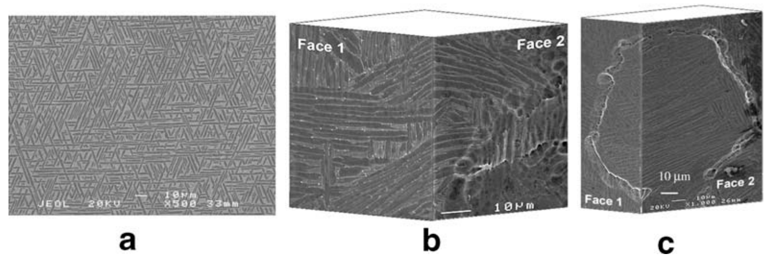

Figure 1. (a) Basketweave microstructure. (b) Windmanstätten microstructure. (c) Equiaxed grain.

were conducted at room temperature, at a load ratio $R = 0.1$, in laboratory air or in a high vacuum of 5×10^{-4} Pa in an environmental chamber. CT specimens, 10 mm thick and 32 mm wide, were pre-cracked until a crack length such as $a/W = 0.25$ was achieved under triangular loading at 20 Hz in accordance with the ASTM-E647 recommendations. The baseline fatigue crack growth rate tests were conducted either under triangular cyclic loading with a 1 s rise and a 1 s fall, i.e. 0.5 Hz, or under dwell loading consisting of a 1 s rise, an 80 s hold period at the maximum stress level and a 1 s fall (1-80-1). The crack length advance was measured using a 100× magnification travelling microscope. Crack length measurements were performed following each crack step of about 0.15 mm.

The tests were conducted at increasing ΔK from an initial value of 12 MPa m$^{1/2}$. The experimental data were plotted on a log–log diagram to give the crack growth rate da/dN with respect to the stress intensity factor range ΔK.

Crack closure was detected by means of the compliance variation method [8] using a strain gauge stuck to the back of each CT specimen, which recorded the evolution of the load displacement loops. A detailed analysis of compliance variations is performed using the differential method initially proposed by Kikukawa [10].

The nominal da/d$N - \Delta K$ data obtained for cyclic loading with and without dwell periods at $R = 0.1$ and at room temperature in air are shown in the log–log diagram of Figure 2. These experimental results clearly show that there is a lower resistance against crack propagation under dwell loading as compared to cyclic triangular loading, with growth rates being about 3–5 times faster in the former case across all the explored ΔK range. To check any possible influence of microstructural variations from one specimen to another, a brief triangular loading sequence was applied during the test with dwell periods; the corresponding crack growth rates were similar to those obtained from the other specimen under merely triangular loading cycles, thus supporting the good reproducibility from one test to another.

After crack closure correction, the effective crack propagation kinetic curves (Fig. 3) still exhibit a faster crack growth under dwell loading; for a given effective ΔK, the crack growth rate is increased by a factor of 2–3. Hence, crack closure cannot account for the increase in the crack growth rate induced by dwell periods, even though the crack closure is slightly more accentuated for triangular loading, which is consistent with rougher crack fracture surfaces.

The results of cyclic tests conducted under a triangular waveform at 0.5 and 20 Hz are plotted in Figure 4 for effective crack propagation. No significant influence of the test frequency was observed. Additional crack growth measurements performed at 0.5 Hz during the test at 20 Hz around $\Delta K = 20$ MPa m$^{1/2}$ yielded growth rates in accordance with those provided by the test run at 0.5 Hz, supporting good reproducibility and the absence of any significant effect of the specimen's microstructure, as found for dwell tests.

The effective crack propagation rates in air and in high vacuum are compared in Figure 5. For growth rates higher than 10^{-7} m cycle^{-1}, the propagation curves for triangular loading in both environments are similar, supporting the absence of any significant effect of atmosphere for this kind of loading. At lower growth rates, da/dN in air becomes faster than that in vacuum, indicating a progressive increase in the effect of environment when the threshold is approached at decreasing ΔK.

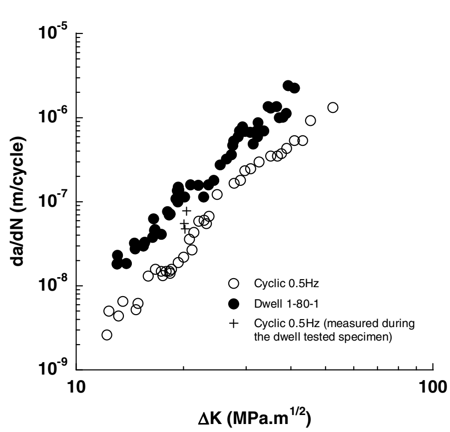

Figure 2. Nominal crack growth curves.

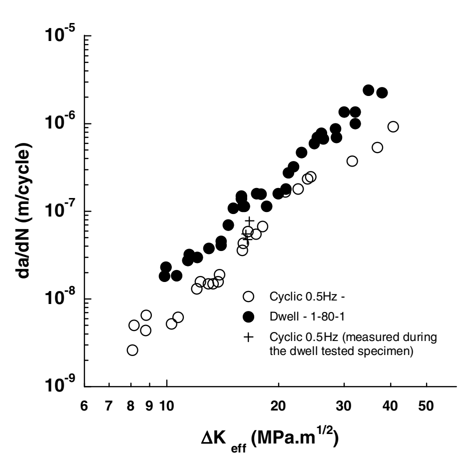

Figure 3. Effective crack growth propagation.